IEEE Access
Multidisciplinary | Rapid Review | Open Access Journal

Received 18 June 2024, accepted 8 July 2024, date of publication 16 July 2024, date of current version 29 July 2024.

Digital Object Identifier 10.1109/ACCESS.2024.3428860

APPLIED RESEARCH

Digital Disturbance Observer Design With Comparison of Different Discretization Methods for Permanent Magnet Motor Drives

KULASH TALAPIDEN[1], YUSSUF SHAKHIN[1], NGUYEN GIA MINH THAO[2], (Senior Member, IEEE), AND TON DUC DO[1], (Senior Member, IEEE)

[1]Department of Robotics and Mechatronics, School of Engineering and Digital Sciences (SEDS), Nazarbayev University, Astana 010000, Kazakhstan
[2]Department of Mechanical, Electrical and Electronic Engineering, Shimane University, Matsue, Shimane 690-8504, Japan

Corresponding authors: Ton Duc Do (doduc.ton@nu.edu.kz) and Nguyen Gia Minh Thao (nguyenthao@ecs.shimane-u.ac.jp)

This work was supported by Nazarbayev University under the Faculty Development Competitive Research Grant Program (FDCRGP) with Grant No.11022021FD2924, and in part by the Research Project of Shimane University under Grant No. FY2024SDGs.

ABSTRACT Control techniques for Permanent Magnet Synchronous Motor (PMSM) drives rely significantly on digital systems, and control system discretization is essential for stability and robustness. While continuous-time analyses are widely employed for stability analysis, generally, they fall short of describing phenomena such as the waterbed effect and understanding system dynamics, especially in servo-drive applications. Consequently, discrete-time systems play a crucial role. The use of discrete-time analysis in digital motion systems of control allows for a more accurate study of system stability while addressing the abovementioned difficulties. Despite the vital role of discrete-time analysis in maximizing stability, robustness, and performance in digital PMSM implementations, there is a significant research gap in the complete analysis and investigation of discrete-time control systems. This research focuses on improving digital disturbance observer (DOB)-based speed control via discrete-time analysis by investigating various discretization techniques. Analyzing widespread discrete-time approaches that rely on analog-to-digital time conversion demonstrates that some strategies outperform others. The paper indicates that constructing a digital DOB-based control utilizing the implicit Adams approach and applying it to PMSMs enhances performance by increasing control accuracy and significantly reducing undershoot when compared to popular discrete-time methods such as Euler's, Tustin, Al-Alaoui, and others. The experimental results show that this chosen discrete-time approach has a significant impact on the efficiency of the PMSM control system. The outcomes of this research highlight the critical relevance of selecting an appropriate discrete-time conversion in improving the performance of a digital DOB motion control system with an application to PMSM drives.

INDEX TERMS Bode integral, digital disturbance observer (DOB), discrete-time methods, motor control, permanent magnet synchronous motor (PMSM), proportional and integral (PI) controller.

I. INTRODUCTION

Disturbances, nonlinearities, and sampling mistakes may all result in a negative impact on motor control. Furthermore, various factors, including friction and cogging torques, as well as uncertain load torque within the speed loop control, can exacerbate the degradation of closed-loop performance in servo drive systems. Each motor control system includes two primary functions: synchronization, which ensures a steady state, and maintaining it during the transient situation [1].

The associate editor coordinating the review of this manuscript and approving it for publication was Feiqi Deng.

In addition, for motor control applications, robustness criteria can be reached using practical disturbance rejection approaches and by implementing an effective control method. The conventional one-degree-of-freedom control approach fails to ensure precise speed-reference tracking and cancellation of load torque, which shows the limitation of the considered approach [2]. Thus, disturbance rejection and its regulation are widespread research subjects in the control theory field, and they are used in real-world applications.

Ohnishi found the Disturbance Observer (DOB) method in the 1980s to ensure the robustness of motion control applications [3]. This method uses the estimated disturbances in order to guarantee exact compensation and also the restoration of the system's operation process. DOB method is widely used in a range of domains, which includes motion control of different applications such as four-rotor helicopters [4], steering wheel mechanisms [5], electric motors [6], robot manipulators with different degree-of-freedom [7], and many others. DOB is an accurate compensator constructed to measure the total impact of external forces on a mechanical structure [8]. Using expected fluctuations for input signals enables it to be more accessible to correct variations across the system and ultimately restore it to its target state of operation. [9]. DOB technique is widely used in speed loop control for Permanent Magnet Synchronous Motor (PMSM) drives for disturbance estimation and prevention, especially for speed-based DOB functions in which disturbances are evaluated by contrasting the measured system velocity with what is predicted in its absence; this evaluation provides the generation of a compensated signal included in the control signal to mitigate the disturbance's impact [10], [11].

Robust motion controllers are often implemented using computers or microcontrollers, and continuous-time analysis and synthesis methods are frequently used for their simplicity in such applications. However, because all physical systems operate in the continuous-time domain by convention, producing control signals directly in the discrete-time domain may not meet performance constraints. In addition, in the high-frequency range, continuous-time analysis falls short of describing certain unanticipated dynamic behaviors and the appearance of the waterbed effect. The difficulty occurs because creating control signals in the discrete-time domain demands an understanding of discrete-time dynamics rather than the system's initial continuous-time dynamics. As a result, investigating discrete-time approaches becomes critical in order to get a more accurate implementation of control systems in servo-drive applications.

In this work, the enhancement of the digital control system for PMSM performance, as well as stability analysis, is shown. Related literature on state-of-the-art analysis of discrete time control methods with an application to servo motor drives is described.

A. RELATED WORKS

Control methods for PMSMs rely significantly on digital systems, including control system discretization, which affects stability and resilience. Previous research, for example, [12], focuses on the augmentation of disturbance observers employing alternative DOB designs, such as for position and acceleration in the discrete-time domain. The move to digital platforms has revealed stability difficulties, influencing decisions regarding design for nominal plants and bandwidth in the control mechanism. In [13], the Bode Integral Theorem was used to demonstrate improved system sensitivity to noise ratio and the presence of the waterbed effect using velocity- and position-based disturbance observer designs. The paper [14] improved the nominal model to address the robust stability issue of DOB. In [15], a speed-adaptive full-order observer's stability and dynamic behavior are examined using Bode and locus diagrams for induction motor drives.

The control analysis of direct current motor parameters using Bode diagrams and Nyquist plots is shown in [16]. In [17], the authors use a bode diagram to optimize controller design for wind turbines with varying speeds. In [18], a discrete-time flux observer is examined for stability and robustness using bode plots in a theoretical application to alternating current (AC) machines. In [19], a discrete-time model of the PMSM drive is applied and studied for exact rotor position control. They developed a discretized back-EMF model to considerably improve the accuracy of the defined problem. The article [20] proposes the Discrete Generalized Bode Criterion (DGBC), a new stability criterion combining Nyquist and Bode criteria. It provides user-friendly assistance in controller design, especially for discrete systems, while accurately defining stability zones. In [21], the authors employed the Euler approximation in the high-frequency region for discrete-time observer design. They contrasted it with classical observer design techniques across various speed ratios, intending to surpass classical DOB designs. Their discrete-time synchronous-frequency adaptive observer (SFAO) provided a significantly more stable reaction, particularly at higher speeds, as proven by their comparison with a surface-mounted PMSM drive.

The impacts of discretization methods on control strategies and the parameters of discretization remain unexplored in existing literature. None of the existing studies have delved into the detailed exploration of various discrete-time techniques specifically aimed at enhancing the performance of motion control systems, particularly when applied to permanent magnet motor drives with a thorough analytical and experimental evaluation.

B. CONTRIBUTION AND EXTENT OF WORK

This work thoroughly studies and analyzes ten discrete-time techniques in the context of control systems managed by digital platforms. Specific methods for reducing ineffective discrete-time approaches have been identified. A thorough Bode Integral analysis was conducted due to insufficient performance and unstable results, particularly in the context of the current application. Notably, a key conclusion in this study focuses on analysis and the identification of

an effective discrete-time technique. This approach can improve stability and performance across a wide range of bandwidths, especially those suitable for motor control systems. Furthermore, the study advises looking at advanced observer designs as a possible technique for investigating larger applications inside motor control systems that could result in increased performance rates. This study thoroughly analyzes and compares numerous discrete-time techniques utilized in control systems for electronic equipment in experiments.

It also investigates the possibility of upgraded observer designs to broaden their use in motor control systems and achieve greater levels of performance and efficiency. Furthermore, it offers practical and theoretical insights that will help advance the field of PMSM motion control and automation. This paper contributes to the field by identifying and advocating for different discrete-time techniques, proposing an inquiry into observer limits, and demonstrating the possibility for improved performance and efficiency in experimental PMSM motion control systems.

The structure of the paper unfolds as follows: Initially, it delves into the implementation of the disturbance observer, conducting its analysis within the continuous-time domain and subsequently comparing it with its discrete-time counterpart. Section III presents a comprehensive examination of ten discrete-time methods, employing the Bode Integral Theorem to ascertain the optimal discrete-time approaches. Additionally, the robustness of the outer loop control system is demonstrated. Section IV elucidates and showcases the experimental results derived from the selected discrete-time techniques, particularly in the PMSM application context. Sections V and VI provide discussion and conclusions, recommendations, acknowledgment of limitations, and suggestions for future research.

II. DISTURBANCE OBSERVER FOR SERVO DRIVE SYSTEM

A. MATHEMATICAL MODEL OF PMSM

The first stage in establishing a motor control system is to create a complete mathematical model [22]. This model demonstrates how distinctive parameters affect the operating setting, notably our speed-based disturbance observer control mechanism. Following is the relevant equation governing the d-q reference frames and electromagnetic torque T_e:

$$\dot{\omega} = \frac{3p^2}{2J}\phi_m i_{qs} - \frac{B}{J}\omega - \frac{p^2}{2J}T_L \tag{1}$$

$$\dot{i_{qs}} = -\frac{R_s}{L_s}i_{qs} - \frac{\phi_m}{L_s}\omega + \frac{1}{L_s}v_{qs} - \omega i_{ds} \tag{2}$$

$$\dot{i_{ds}} = -\frac{R_s}{L_s}i_{ds} - \frac{\phi_m}{L_s}\omega + \frac{1}{L_s}v_{ds} - \omega i_{qs} \tag{3}$$

$$T_e = \frac{3}{2}Z_p K_e i_q \tag{4}$$

where ω - the rotor's speed, p - number of poles, i_{ds} and i_{qs} stator current for corresponding frames, v_{qs}, v_{ds} - stator voltages, ϕ_m - magnetic flux linkages, B - stator resistance, J - inertia, T_L - load torque, L_s and R_s stator's inductance and resistance, I_q - phase current, Z_p - pole pairs

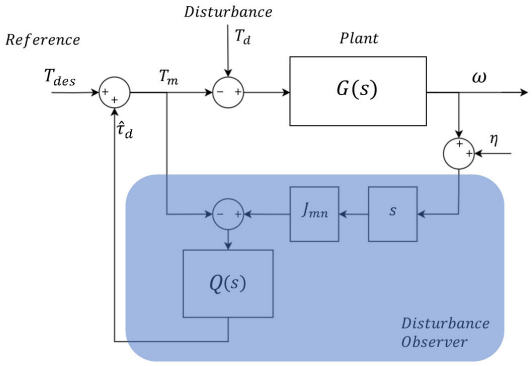

FIGURE 1. Block diagram of speed-based disturbance observer in continuous-time domain.

B. SPEED-BASED DISTURBANCE OBSERVER ANALYSIS IN CONTINUOUS-TIME DOMAIN

The DOB technique is extensively employed in speed loop control for PMSMs, with the purpose of assessing and reducing system disturbances [3]. The speed-based DOB, for instance, detects disturbances by comparing the system's actual speed ratio to the target value in the absence of a perturbation. Fig. 1 depicts a block diagram of a continuous-time domain speed-based DOB, demonstrating the interrelationship between the servo dynamics of the PMSM and the DOB. In this figure, J_m, J_{mn} – inertia and its nominal, s – Laplace variable for continuous time domain, g_B – bandwidth of the speed-based DOB, $\widehat{\tau}_d$, τ_d and η – total disturbance, input disturbance and noise, w, $\dot{w}$ – speed and acceleration of PMSM. A transfer function is used in control engineering to describe the connection between the input and output values of a linear time-invariant system [20]. The following equation will be derived for the transfer function of the motion control system:

$$G_{T_{des}}(s) = \frac{G(s)G_n(s)}{G_n(s) + Q(s)(G(s) - G_n(s)} \tag{5}$$

$$S(s) = \frac{G_n(s)(1 - Q(s)}{G_n(s) + Q(s)(G(s) - G_n(s))} \tag{6}$$

$$T_\eta(s) = \frac{G(s)Q(s)}{G_n(s) + Q(s)(G(s) - G_n(s))} \tag{7}$$

$$L_v(s) = \frac{G(s)Q(s)}{G_n(s)(1 - Q(s))} \tag{8}$$

where $G(s)$ - system's plant; $G_n(s)$ - system's nominal; $Q(s)$ - low pass filter. In particular, the transfer function of DOB in the context of the Inner Loop is expressed as follows:

$$\omega(s) = G_{T_{des}}(s)T_{des} + J_m S(s)T_d + T_\eta(s)\eta \tag{9}$$

where sensitivity transfer function is $S(s) = \frac{s}{s+g_B\alpha}$ and parameter uncertainties $\alpha = \frac{J_{mn}}{J_m}$. Complementary sensitivity function $T_\eta(s) = \frac{g_B\alpha}{s+g_B\alpha}$, phase-lead/lag compensator $G_{T_{des}} =$

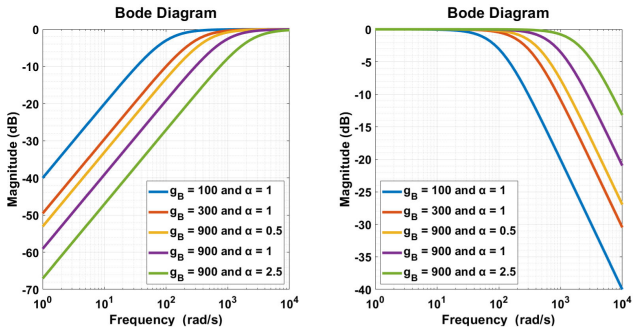

FIGURE 2. Frequency response of speed-based disturbance observer in continuous time domain.

$\frac{g_B+s}{J_m(s^2+sg_B\alpha)}$ and the control system's open-loop transfer function is $L_v = \frac{g_B\alpha}{s}$.

The analysis of system stability and resilience can be facilitated by using the Bode integral theorem [21], which can be derived by:

$$\int_0^\infty \ln|S(e^{j\omega})|\,d\omega = -\frac{\pi}{2}\lim_{s\to\infty} sL_v(s) + \pi\sum_i Re(p_i)$$
$$= -\frac{\pi}{2}\alpha g_B \tag{10}$$

The speed-based DOB evaluation in continuous time using the Bode Integral yields no high sensitivity quantities. The Bode Integral result shows that the system does not suffer from the waterbed effect, suggesting a stable system with no high sensitivity quantities. According to [12], continuous-time disturbance observers exhibit oscillatory behavior, leading to system instability as the plant's bandwidth grows. Evaluating the dynamic properties of DOB-based, robust digital motion controllers highlights the limitations of continuous-time analytical methods.

According to [23], discrete-time implementations limit the DOB's bandwidth stability. The higher bandwidth of the DOB may result in undesired dynamic aspects, such as decreased performance and stability. As a result, the next step is to assess the DOB's robustness using a mechanism for transitioning the system from the continuous to the discrete-time domain.

III. DISCRETIZATION METHODS

Discretization is the process of converting a continuous-time control framework into a discrete-time system appropriate for use with digital computers. Discretization methods are crucial in control systems, influencing precision, stability, and efficiency [24]. The input signal is sampled at regular intervals, and its behavior is determined using a discrete-time framework, transforming the continuous-time control system into a mathematically understandable discrete-time form. According to [12], discretization is crucial in determining the stability of control systems for electrical system applications.

Different approximation techniques influence the system's performance behavior. In [25], they analyze Zero Order Hold (ZOH), Backward difference, and bilinear transformation on the PI position controller with an application to the DC motors. In [26], the authors present an investigation of several discretization approaches for evaluating the elastodynamic wave propagation performance, in which they show the boundary limitations of approximations. The implementation and evaluation of adaptive and learning control techniques on DC motors show that the performance improves using first-order hold discretization and a large sample time [27].

TABLE 1. Discrete time Methods and their equations, $\frac{1}{s}$.

Discrete-Time-Method	General Form
Forward Rectangular Rule	$\frac{T_s}{z-1}$
Backward Rectangular Rule	$\frac{T_s z}{z-1}$
Bilinear (Tustin) Approximation	$\frac{T_s}{2}\frac{z+1}{z-1}$
Implicit Adams Second Order	$\frac{3T_s}{2}\frac{1-\frac{z}{3}}{1-z^{-1}}$
Simpson's Numerical Integration	$\frac{T_s}{3}\frac{1+4z^{-1}+z^{-2}}{1-z^{-2}}$
Al-Alaoui Method	$\frac{7T_s}{8}\frac{1+\frac{1}{7}z^{-1}}{1-z^{-1}}$
Upward Parabolic Integration	$\frac{T_s}{3}\frac{2+z^{-1}}{1-z^{-1}}$
Downward Parabolic Integration	$\frac{T_s}{3}\frac{1-z^{-1}}{2+z^{-1}}$
Halijak Second Order Method	$\frac{T_s^2 z}{(z-1)^2}$
Tick Integration Rule	$\frac{T_s}{2.7902}\frac{1+3.5804z^{-1}+z^{-2}}{1-z^{-2}}$

The backward rectangular rule is a numerical integration technique used extensively in signal processing and control systems. It is widely used to approximate the s-to-z transform in discrete-time systems [28]. The Tustin approximation is a digital filtering technique that involves comparing two filters in continuous time to discrete time. This strategy is referred to as the bilinear approximation approach [29]. The implicit Adams second-order hold approach is a numerical method for solving ordinary differential equations. An integral value is estimated using a numerical integration approach known as Simpson's rule. The Al-Alaoui technique [30] is a numerical approach for solving nonlinear algebraic equations. Upward Parabolic Integration is a numerical approach for discretizing control systems, an extension of the trapezoidal rule, and a popular way to approximate integrals. As well as Downward Parabolic Integration is a numerical technique used in discretizing control systems, referenced as an extension of the trapezoidal rule. It's recognized as a prevalent method for approximating integrals within control system contexts, mentioned in literature as a valuable tool for numerical integration [31]. Halijak discretization is used to digitally reproduce all-pass, notch, and high-pass filters, even if they have zero initial input signals [32]. Simpson's Rules are approaches for estimating a definite integral within a limited interval, $t_0 \le t \le t_0 + T\delta$, by fitting an m_{th} order the polynomial via m values of the function inside that interval and calculate the area under this polynomial curve [33]. Among the discretization approaches evaluated, the Tick integration rule stands out for its ability to handle

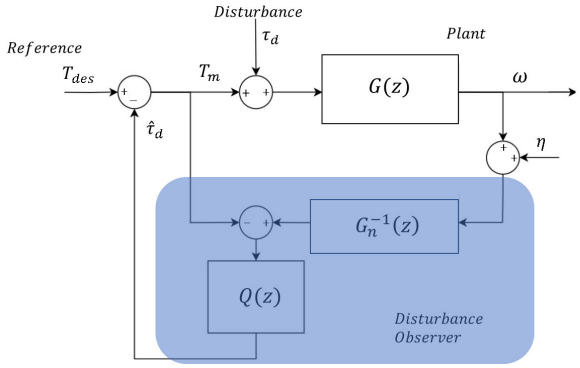

FIGURE 3. Block diagram for inner loop speed-based disturbance observer in discrete time domain.

non-uniform data sampling. It provides a possible advantage in situations with irregularly spaced data points [34].

Upper-defined existing transformations were employed specifically to convert the Laplace transform variable from the 's' domain to the 'z' domain of the z-transform. The next sections will look at ten of the most common and commonly utilized approximation approaches. The purpose of this analysis is to elucidate the trade-offs between robustness and stability when using these discretization approaches to develop motion control systems, as well as to provide insights into their practical application in dynamic systems. As stated in Table 1, the following investigation focuses on discrete-time approaches and their application for the speed-based disturbance observer.

A. STABILITY ANALYSIS OF DIGITAL DISTURBANCE OBSERVER

Fig.3 depicts a block diagram for speed-based DOB-based control of the PMSM system. The general form of the transfer function of the control system can be found:

$$\omega(z) = G_{T_{des}}(z)T_{des} + J_m S(z)T_d + T_\eta(z)\eta \tag{11}$$

where T_{des} - command input, T_d - external disturbance, η - sensor noises. Representation of system's uncertainties the following parameter $\alpha = \frac{J_{mn}}{J_m}$ is applied.

From the conventional control theory, the stability of a discrete-time system can be measured by studying the positions of its eigenvalues in the z-plane. According to [35] the following eigenvalue criterion can be used for judging the system's stability:

$$\max(|x_i|) \leq 1, \quad i = 1, 2, 3, \ldots, n \tag{12}$$

where x_i is an eigenvalue of the discrete-time system.

Table 3 compares multiple discrete-time approaches for Open Loop BIBO analysis, emphasizing significant variances in the absolute value of eigenvalues, damping, frequency, and stability properties. Most methods, including the Forward Rectangular Rule, Backward Rectangular Rule, Bilinear (Tustin) Approximation, and others, have similar characteristics, with magnitudes ranging from 0.98 to 1.0, (12) critical damping ratios of 1.0, and frequencies ranging from 1.24 to 1.45 rad/TimeUnit, indicating stable behavior with minimal attenuation or amplification. Exceptions include the Simpson's Numerical Integration and the Tick Integration Rule, which exhibit higher frequencies (3.14 rad/TimeUnit) and greater damping ratios (1.33 and 1.13, respectively), indicating over-damping and unstable behavior.

The Bode Integral (13) formula in the discrete-time domain can be found as follows:

$$\int_0^{2\pi} \ln|S(e^{j\omega})|\, d\omega = 2\pi(-\ln|\lim_{z\to\infty} L(z) + 1| + \sum_i \ln|p_i|) \tag{13}$$

Suppose the open-loop transfer function exhibits precisely one higher degree in the denominator compared to the numerator. In that case, there is a penalty in waterbed effect to reduce or remove sensitivity peak with the following $-\ln|\lim_{z\to\infty} L(z) + 1|$ [36], otherwise this expression becomes 0 and suffers from waterbed effect.

Now, let us delve into the examination of the speed-based disturbance observer's stability in control of PMSM using ten discrete-time techniques in this section of the paper. Table 2 indicates the transfer function of low-pass filter sensitivity (6) and complementary sensitivity (7) functions; it also displays the calculation of the open-loop transfer function (8) and Bode Integral (13) results in the discrete-time domain. In [37], the connection of feedback control from Bode Integral (13) is shown. It describes that the influence of disturbances is decreased in the case that $|S| < 1$ and in the frequency range of $|S| > 1$ noise affects the system's stability. The inner-loop controllers' phase range and the velocity-based DOB's bandwidth are determined by noise sensitivity and the waterbed effect limit. As the DOB's bandwidth rises, the waterbed effect might lead the control system to exhibit an unstable response. In two out of ten approximations, bode integral results show a waterbed effect, which will cause instability issues in the high bandwidth range.

To evaluate different discretization techniques' ability to suppress noises in the high-frequency range, the evaluation of sensitivity and complementary sensitivity transfer functions is discussed. In motor drive applications, the sensitivity transfer function describes systems disturbance attenuation. It essentially assesses the system's robustness and ability to reject disturbances, which is critical for retaining accurate control over motor speed and position despite load or supply voltage variations. On the other hand, the complementary sensitivity transfer function measures how well the system suppresses the noise. This analysis will help us to understand the DOB system's stability and robustness against disturbances and noise, particularly in the high-frequency range.

Fig. 4 shows the frequency response of each method's sensitivity transfer function on the left side. Here, the discrete-time methods are compared starting from the bandwidth of the system $g_B = 100$ and parameter uncertainties $\alpha = 1$ until the $g_B = 900$ and $\alpha = 2.5$. In control

TABLE 2. Discrete-time-method transfer function.

Discrete-Time-Method	Sensitivity Function, $S(z)$	Complementary Sensitivity Function, $T_\eta(z)$	Open Loop Transfer function, $L(z)$	Bode Integral Results
Forward Rectangular Rule	$\frac{z-1}{z-1+g_bT_s\alpha}$	$\frac{g_bT_s\alpha}{z-1+g_bT_s\alpha}$	$\frac{g_bT_s\alpha}{z-1}$	0
Backward Rectangular Rule	$\frac{z-1}{z(1+g_bT_s\alpha)-1}$	$\frac{g_bT_sz\alpha}{z(1+g_bT_s\alpha)-1}$	$\frac{g_bT_sz\alpha}{z-1}$	$g_BT_s\alpha$
Bilinear (Tustin) Approximation	$\frac{2(z-1)}{2(z-1)+g_bT_s\alpha(1+z)}$	$\frac{g_bT_s(z+1)\alpha}{2(z-1)+g_bT_s\alpha(1+z)}$	$\frac{g_bT_s(z+1)\alpha}{2(z-1)}$	$\frac{g_BT_s\alpha}{2}$
Implicit Adams Second Order Hold	$-\frac{2(z-1)}{2(1-z)+g_bT_s\alpha(1-3z)}$	$\frac{g_bT_s\alpha(3z-1)}{2(1-z)+g_bT_s\alpha(1-3z)}$	$\frac{g_bT_s(3z-1)\alpha}{2(z-1)}$	$\frac{3g_BT_s\alpha}{2}$
Simpson's Numerical Integration	$\frac{3(z^2-1)}{3(z^2-1)+g_BT_s\alpha(1+z^2\alpha+4z)}$	$-\frac{g_bT_s\alpha(z^2+4z+1)}{3(z^2-1)+g_BT_s\alpha(1+z^2\alpha+4z)}$	$\frac{g_bT_s(z^2+4z+1)\alpha}{3(z^2-1)}$	$\frac{g_BT_s\alpha}{3}$
Al-Alaoui Method	$\frac{8(z-1)}{8(z-1)+g_BT_s\alpha(1+7z)}$	$\frac{g_BT_s\alpha(7z+1)}{8(z-1)+g_BT_s\alpha(1+7z)}$	$\frac{g_BT_s\alpha(7z+1)}{8(z-1)}$	$\frac{7g_BT_s\alpha}{8}$
Upward Parabolic Integration	$\frac{3(z-1)}{3(z-1)+g_BT_s\alpha(1+2z)}$	$\frac{g_BT_s\alpha(2z+1)}{3(z-1)+g_BT_s\alpha(1+2z)}$	$\frac{g_BT_s\alpha(2z+1)}{3(z-1)}$	$\frac{2g_BT_s\alpha}{3}$
Downward Parabolic Integration	$\frac{3(z-1)}{3(z-1)+g_BT_s\alpha(2+z)}$	$\frac{g_BT_s\alpha(z+2)}{3(z-1)+g_BT_s\alpha(2+z)}$	$\frac{g_BT_s\alpha(z+2)}{3(z-1)}$	$\frac{g_BT_s\alpha}{3}$
Halijak Second Order Method	$\frac{(z-1)^2}{z(g_BT_s^2\alpha+z-2)+1}$	$\frac{g_BT_s^2z\alpha}{z(g_BT_s^2\alpha+z-2)+1}$	$\frac{g_BT_s^2z\alpha}{(z-1)^2}$	0
Tick Integration Rule	$\frac{2.8(z^2-1)}{2.8(z^2-1)+g_BT_s\alpha(1+z^2+3.6z)}$	$\frac{g_BT_s\alpha(z^2+1.8z+1)}{2.8(z^2-1)+g_BT_s\alpha(1+z^2+3.6z)}$	$\frac{g_BT_s\alpha(z^2+1.8z+1)}{2.8(z^2-1)}$	$\frac{g_BT_s\alpha}{2.8}$

TABLE 3. Discrete-time-method open loop BIBO analysis.

Discrete-Time Method	Magnitude	Damping	Frequency rad/TimeUnit
Forward Rectangular Rule	0.98	1.0	1.26
Backward Rectangular Rule	0.98	1.0	1.24
Bilinear (Tustin) Approximation	0.98	1.0	1.25
Implicit Adams Second Order Hold	0.98	1.0	1.45
Al-Alaoui Method	0.99	1.0	1.25
Upward Parabolic Integration	0.98	1.0	1.25
Downward Parabolic Integration	0.98	1.0	1.25
Simpson's Numerical Integration	1.02	1.33	3.14
Halijak Second Order Method	1.0	2.48	1.25
Tick Integration Rule	1.01	1.13	3.14

TABLE 4. Discrete-time-method transfer function.

Discrete-Time Method	Discrete Time Order	Waterbed Effect	Open Loop Stability
Forward Rectangular Rule	1	Yes	BIBO Stable
Backward Rectangular Rule	1	No	BIBO Stable
Bilinear (Tustin) Approximation	1	No	BIBO Stable
Implicit Adams Second Order Hold	1	No	BIBO Stable
Al-Alaoui Method	1	No	BIBO Stable
Upward Parabolic Integration	1	No	BIBO Stable
Downward Parabolic Integration	1	No	BIBO Stable
Simpson's Numerical Integration	2	No	BIBO Unstable
Halijak Second Order Method	2	Yes	BIBO Stable
Tick Integration Rule	2	No	BIBO Unstable

systems and signal processing, bandwidth refers to the range of frequencies that a system or component can work successfully. Using these defined values, it is possible to systematically test the efficacy of various discretization algorithms over a wide frequency range.

Such that Halijak second-order and forward rectangular rule methods have sensitivity peaks in the middle and high frequency ranges due to the waterbed effect. In downward parabolic integration, the bode integral equation shows that it cannot entirely decrease the sensitivity peaks. Moreover, the others do not suffer from the waterbed effect. However, implicit Adams and upward parabolic integration have better disturbance attenuation in middle and high-frequency ranges.

As the complementary sensitivity transfer function (right side of Fig.4) shows the system's ability to attenuate noise, it shows that discretization methods have similar performance. The noise of speed measurement is attenuated less as the design parameters decrease. For example, the system demonstrates enhanced noise suppression capabilities when $g_B = 100$ and $\alpha = 1$. When a frequency response plot is far from 0, it indicates significant amplification or attenuation of signals at specific frequencies, demonstrating the system's strong frequency-dependent responding characteristics. While, with the frequency range of $g_B = 900$ and $\alpha = 2.5$, Halijak's order method and downward parabolic integration show a lower ability to suppress noise. Other methods, such as the bilinear approach and implicit Adams, are highly effective in attenuating the noise of the measurement in the high-frequency range.

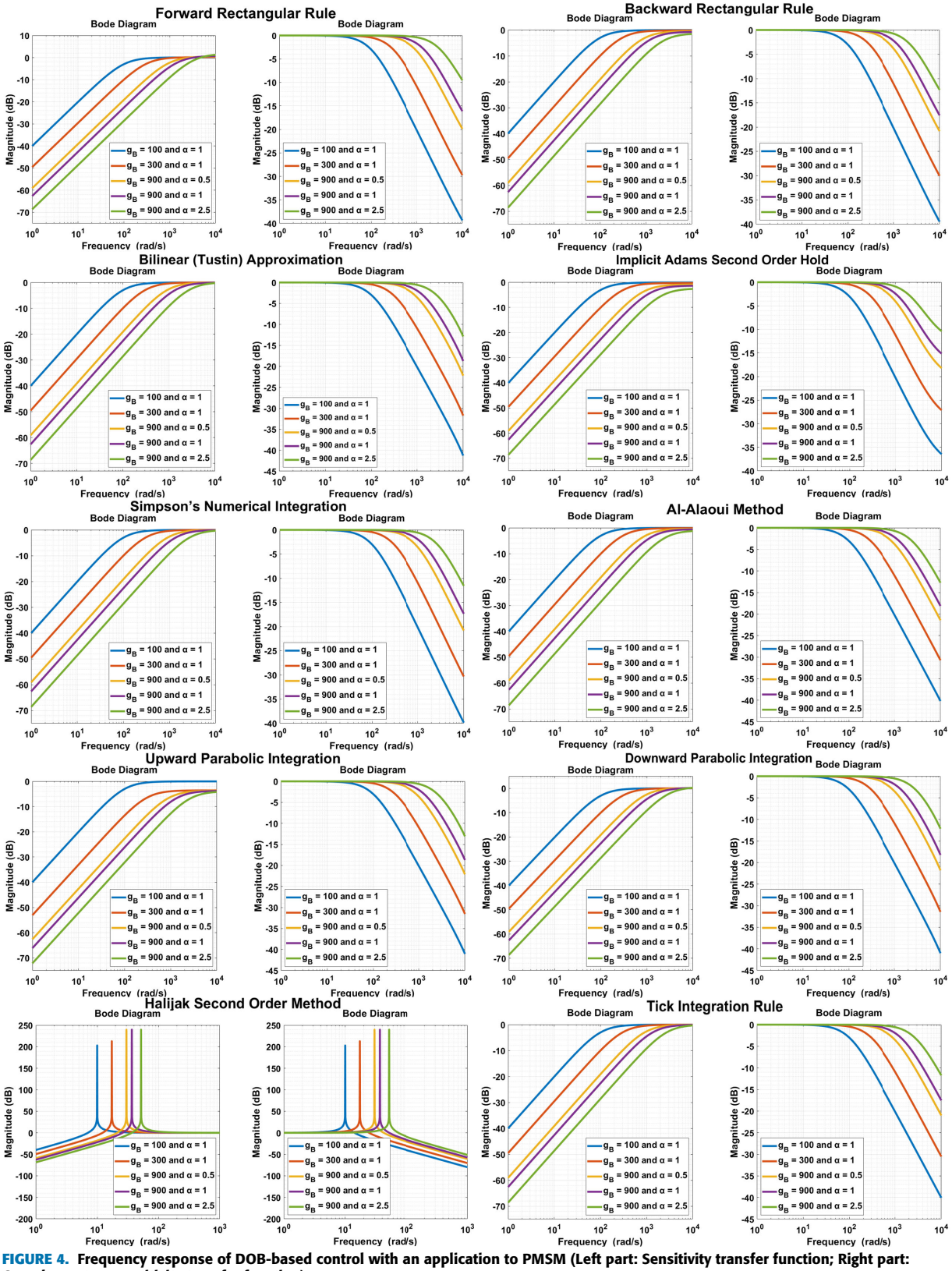

FIGURE 4. Frequency response of DOB-based control with an application to PMSM (Left part: Sensitivity transfer function; Right part: Complementary sensitivity transfer function).

Table 4 compares various discrete-time approaches, with a particular emphasis on the waterbed effect as well as open-loop stability. Because of the importance of BIBO (Bounded Input Bounded Output) stability and the ability to

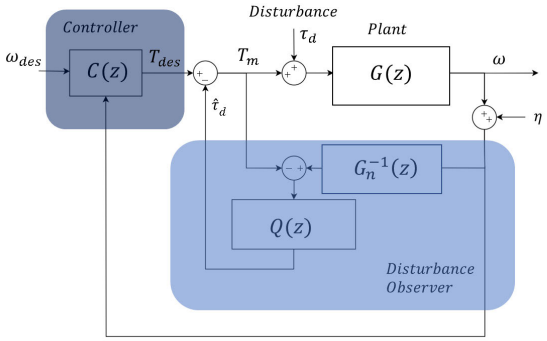

FIGURE 5. Disturbance observer-based control algorithm with application to PMSM.

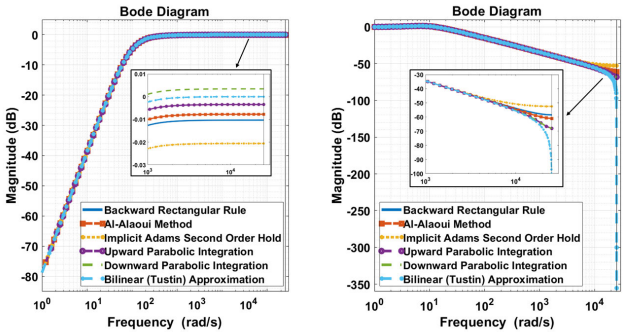

FIGURE 6. Frequency response of speed-based dob applying six distinctive approaches with $g_B = 100$ and $\alpha = 1$.

characterize system behavior using Markov variables, BIBO stable systems are a basic topic in control theory [38]. While maintaining BIBO stability, the Forward Rectangular Rule and Halijak second-order method exhibit a waterbed effect. The Backward Rectangular Rule, on the other hand, exhibits no waterbed effect and remains BIBO stable. The Bilinear (Tustin) Approximation, Implicit Adams Second Order Hold, Al-Alaoui Method, Upward Parabolic Integration, and Downward Parabolic Integration all have no Waterbed Effect and keep BIBO stable. On the other hand, Simpson's numerical integration and Tick Integration Rule reveal no waterbed effect but cause BIBO instability.

Based on the waterbed effect and open loop stability, it is clear that four options will be discarded for further inquiry and analysis due to their limits in ensuring stable behavior and performance within the system. The purpose of this part is to explain the decision to focus on techniques that exhibit BIBO stability as well as the absence of the Waterbed Effect, emphasizing the importance of strong and dependable discrete-time methods for future research in this sector.

B. DIGITAL DOB-BASED SPEED CONTROL STRATEGY FOR PMSM DRIVE

Outer-loop control in PMSM is primarily concerned with altering the motor's speed, position, or acceleration. This often involves utilizing an encoder to measure the motor's speed or position and comparing it to the desired result. The presence of a closed loop has a significant effect on stability. Fig. 5 demonstrates the control of PMSM using a proportional integrator derivative (PID) control system and a speed-based DOB.

PID control systems are a typical closed-loop control technique used in PMSM control algorithms. Fig.5 depicts the block diagram for PMSM's digital speed control system, which includes a feedback controller designated $C(z)$ and a low-pass filter $Q(z)$. PID and DOB tuning are performed to improve system performance and robustness. Different methodologies for designing in the discrete-time domain might be utilized for the PI controller part.

However, in this study, in order to focus on DOB performance and its robustness, we preserved the speed controller design using Bilinear Approximation throughout all systems. Such that the speed controller equation is synthesized as follows:

$$C(z) = K_p + \frac{K_p}{T_n}\frac{2(z-1)}{T_s(z+1)} \tag{14}$$

in which servo drive controller gains are [0.057, 0.5] for K_p, and [0.04, 1] for T_n. The resulting equation of the speed control system is as follows:

$$\omega = G_{\omega_{des}}(z)\omega_{des}(z) + G_{\tau_d}(z)\tau_d + G_\eta(z)\eta(z) \tag{15}$$

Outer loops for sensitivity and complementary sensitivity functions can be obtained as:

$$S_o(z) = \frac{G_n(1-Q)+GQ}{G_n(1-Q)+GQ+G_nGC} \tag{16}$$

$$T_o(z) = \frac{GG_nC}{G_n(1-Q)+GQ+GG_nC} \tag{17}$$

According to (13), closed-loop performance influences the stability of motion control strategies for PMSM. Next, the Bode Integral Theorem is used for stability analysis of the servo drive control algorithm. Because all systems do not have unstable poles, the Bode Integral equation is simplified to the following form:

$$\int_0^{2\pi} \ln(|S_o(e^{j\omega})|)\, d\omega = -2\pi \ln|1 + \lim_{z\to\infty} L(z)| \tag{18}$$

These (16)-(17) highlight the impact of bandwidth and α on the sensitivity and complementary sensitivity functions, emphasizing the importance of constructing digital DOBs in defining the performance and stability of a speed control system. This study attempts to investigate the system's robustness in the control system. Fig. 6 shows comprehensive frequency response visualizations, illustrating the sensitivity S_o and complimentary sensitivity T_o functions for outer loops utilizing speed-based DOB.

The results show a consistent pattern across all techniques, with stable responses that converge to zero. In terms of sensitivity transfer function analysis, the techniques perform similarly, with the exception of the implicit Adams approach, which is somewhat better at damping disturbances, showing enhanced system responsiveness. This comparison gives

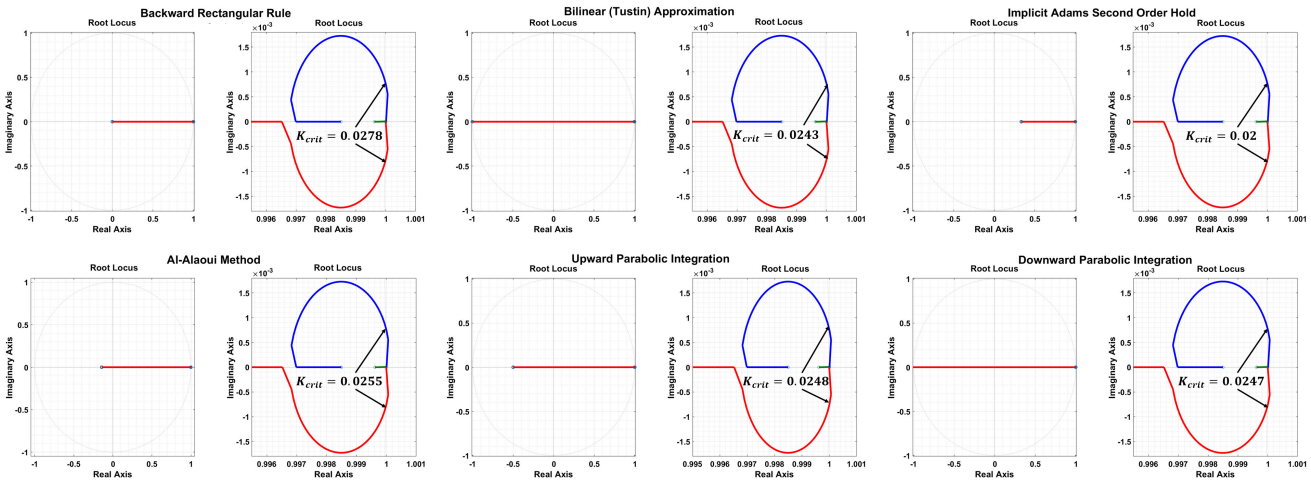

FIGURE 7. Root locus of speed-based disturbance observer: applying six distinctive discrete-time approaches with $g_B = 100$ and $\alpha = 1$.

TABLE 5. PMSM technical characteristics.

PMSM Parameter	Value & Unit
Rated speed	2500, rpm
Rated torque	0.97, Nm
Peak Torque	4, Nm
Constant Torque	0.41, Nm
DC link Voltage	200, V
Peak Current	12, A
Winding Inductance	8.6, mH
d-axis and q-axis Inductance	$2/3 \cdot L_s$, H
Winding Resistance	4.74, Ω
Permanent Magnet Flux	0.089, Wb
Number of Poles	8
Nominal Inertia of the Rotor	0.000033, kg· m^2
Frequency of Gate Pulse Generator	10, kHz

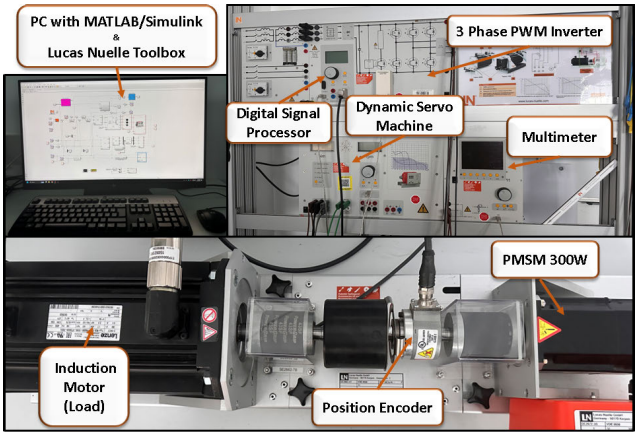

FIGURE 8. Experimental setup for the motion control system.

light on the various performance characteristics of different approaches, which are crucial for evaluating their usefulness in real-world applications inside control systems. The most noticeable distinction between discrete time approaches is the complimentary sensitivity transfer function (Fig. 6, right side) response, which implies speed reference tracking. All approaches provide effective reference tracking at low frequencies, with deterioration at middle and high frequencies. Adams discretization has slightly greater tracking skills than the others.

The stability constraints can be observed in the root loci of speed-based DOB employing six distinctive discrete-time strategies with respect to α. Fig. 7 depicts the lower bound of parameter mismatch of the six techniques. Implicit Adams method shows a broader range for parameter mismatch by having a lower bound equal to 0.02. While the stricter constraint can be needed for the backward rectangular rule with the lower bound equal to 0.0278, another method that also requires such constraints with the lower bound 0.0255 is the Al-Alaoui method.

The analysis provides beneficial insights into system stability and performance. With the closed-loop analysis in the discrete-time domain, the assessment and enhancement of the motion control system can be guaranteed in comparison with the continuous time domain analysis.

IV. EXPERIMENTAL RESULTS

A. EXPERIMENTAL SETUP

The experimental phase of this research was conducted using a 300 W PMSM setup manufactured by Lucas-Nuelle GmbH, which incorporates a digital signal processor, as depicted in Fig. 8. This arrangement in Fig. 8 showcases the configuration utilized to regulate the PMSM's speed. The setup comprises a surface-mounted PMSM connected to a 1024-pulse sequential motion encoder and a servo machine controlled by ActiveServo software, serving as a load. Detailed characteristics of the PMSM are outlined in Table 5 for reference.

TABLE 6. Experimental parameters.

Parameter	Scenario 1	Scenario 2	Scenario 3
Set Speed, rpm	2000	2000	2000
Mechanical Offset	34	34	34
Bandwidth, g_B	10	20	20
Parameters Uncertainty, α	1	1	2
Load, Nm	0.8	0.8	0.8

B. EXPERIMENTAL COMPARISON OF DISCRETE-TIME METHODS

Six discrete time approximations are used to evaluate the performance and stability of the PMSM's control strategy (Table 4). Experiments have been conducted with the conditions in Table 6. This study established the proportional-integral (PI) controller gains at $K_p = 0.057$ and $T_n = 0.4$. Additionally, we fine-tuned the DOB parameters (bandwidth and parameter uncertainty) to assess the effectiveness of the discrete control system based on DOB (referenced in Table 6). Consequently, for a comprehensive evaluation, we conducted three distinct cases to thoroughly assess the motion control system's performance. The motor's reference speed is initially set to 2000 rpm in the experimental setup. Once the motor reaches a steady speed, an unforeseen load torque is introduced to the PMSM drive at 0.3 seconds. To gauge the performance of these systems, various metrics, such as the Integral of Absolute Error (IAE), Integral of Time Absolute Error (ITAE), and Root Mean Square Error (RMSE), were utilized.

In a complete experimental examination of speed control employing six discrete-time approaches, the insights derived from Fig. 10 are based on specific conditions: a system bandwidth of $g_B = 10$ and parameter uncertainties represented by $\alpha = 1$. The exhibited speed responses demonstrate the efficiency of each discrete-time approach in steering the motion control system, ensuring that the desired speed of 2000 rpm is maintained despite disturbances and nonlinearities. Notably, the Al-Alaoui-based control emerges as the dominant, with superior speed response, as seen by reduced undershoot and increased settling time. In comparison, the backward rectangular rule lags far behind, demonstrating markedly lower performance as evidenced by significantly higher undershoot compared to the other options.

Analyzing the current response in Fig. 9, it becomes evident that the Tustin approximation exhibits a slightly superior performance, achieving a value of 5.88 A. Interestingly, the six discrete-time methods demonstrate nearly comparable performances, characterized by minimal variations and the highest value recorded at 6.212 A, attributed to upward parabolic integration. This close similarity in the performance of the discrete-time methods underscores their comparable effectiveness in handling system dynamics, with only marginal distinctions in current response magnitudes.

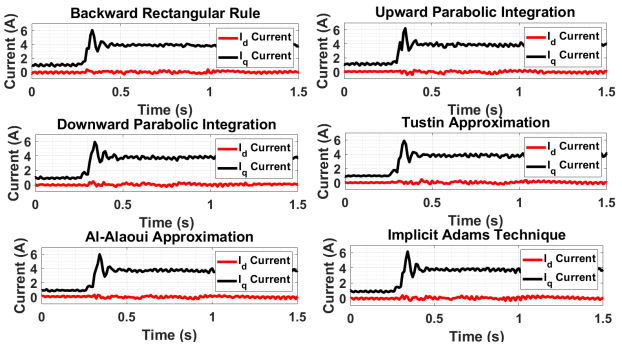

FIGURE 9. Scenario 1: Current response using six discrete-time approximations with $g_B = 10$ and $\alpha = 1$.

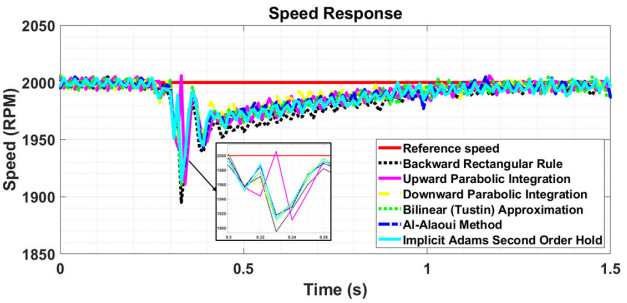

FIGURE 10. Scenario 1: Speed tracking findings using six discrete-time approximations with $g_B = 10$ and $\alpha = 1$.

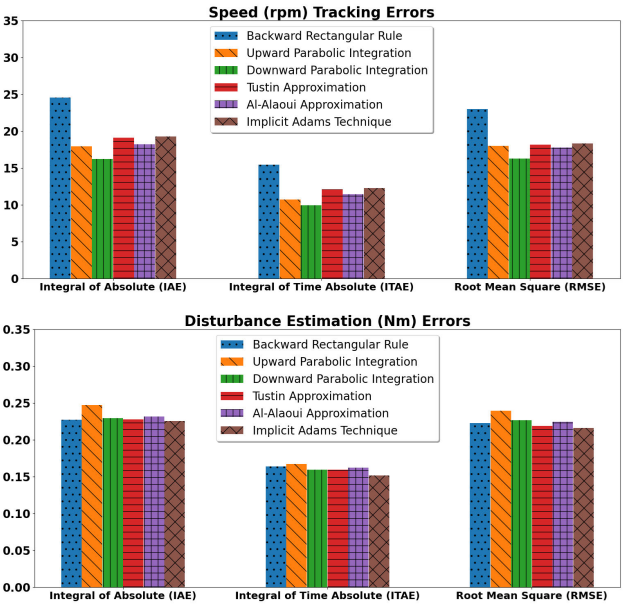

FIGURE 11. Scenario 1: Estimation errors of load change for speed tracking (upper part) and disturbance estimation (bottom part) using six discrete-time approximations with $g_B = 10$ and $\alpha = 1$.

Fig.11 (top part) shows the estimation errors of the digital DOB control system utilizing the defined approximations. The use of downward parabolic integration results in a slight performance improvement. In ITAE error estimation, speed

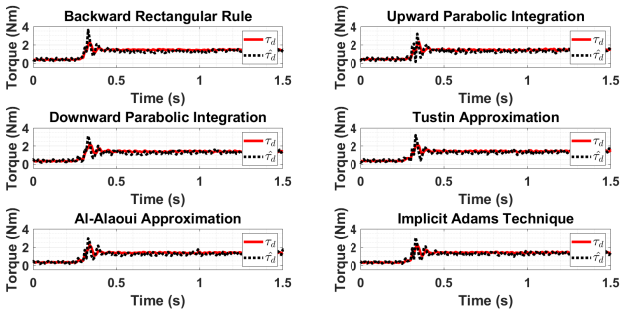

FIGURE 12. Scenario 1: Total disturbance estimation using six discrete-time approximations with $g_B = 10$ and $\alpha = 1$.

tracking errors obtain the lowest value of 9.94, while the backward rectangular rule has the highest value of 15.4. The Integral Absolute Error for downward parabolic integration is 16.195, while the highest value is 24.53 for the backward rectangular rule; nonetheless, the other four procedures have values in the range of 18 to 19. The Root Mean Square Error (RMSE) indicates a consistent performance order among the methods, with the smallest error at 9.95 and the highest at 15.41. In the lower part of Fig. 11, disturbance estimation reveals nearly identical performances with minimal differences among the approximations. Slightly superior disturbance estimation is observed for the implicit Adams technique, but overall, the variations between the usage of different approximations are minimal.

Figure 12 provides a visual depiction of the disturbance estimation capabilities of each system, offering insights into their capacity to monitor and respond to disturbances over time. Although slight variations between methods are discernible, the differences in values are minimal, ranging from 3.6 to 2.96 Nm. Notwithstanding these subtle distinctions, the graphical representation of the data suggests that, on average, all six techniques showcase comparable performance. They consistently track in alignment with the speed reference, emphasizing the robust disturbance estimation capabilities inherent in each evaluated method. This visual insight underscores the overall reliability and effectiveness of the techniques in maintaining stability and responsiveness in the face of disturbances.

In the following case (Scenario 2), the experiment is conducted with an increased bandwidth of $g_B = 20$ while maintaining the same parameter uncertainties at $\alpha = 1$. The implicit Adams approach demonstrates superior performance in speed response (Fig. 14), showcasing minimal undershoot. It also exhibits the least disturbance estimation error at 3.7 Nm (Fig. 15). Moreover, the upward parabolic integration displays commendable performance in both speed tracking and disturbance estimation, achieving a value of 4.1. However, when the bandwidth is increased in both scenarios (see Figs. 14 and 15), the backward rectangular rule consistently displays the poorest performance. It exhibits the highest disturbance estimation error at 5.579 Nm and

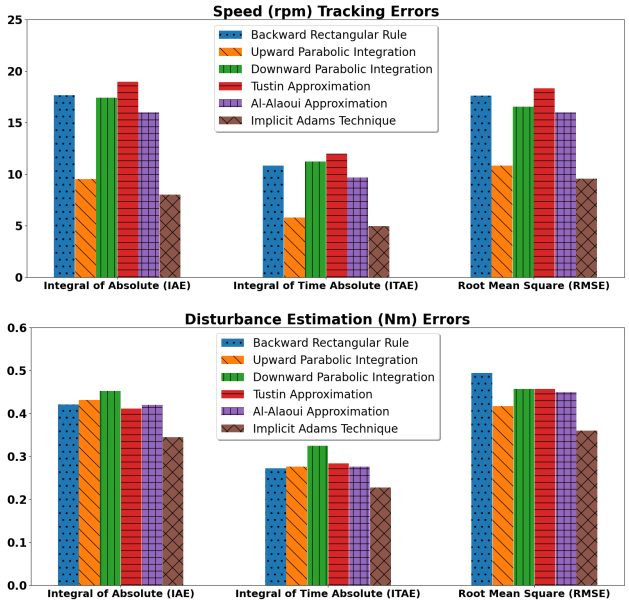

FIGURE 13. Scenario 2: Speed tracking findings using six discrete-time approximations with $g_B = 20$ and $\alpha = 1$.

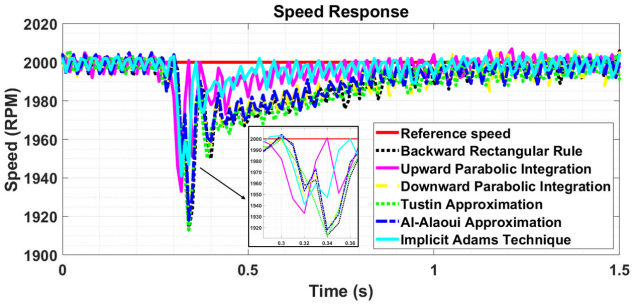

FIGURE 14. Scenario 2: Speed tracking findings using six discrete-time approximations with $g_B = 20$ and $\alpha = 1$.

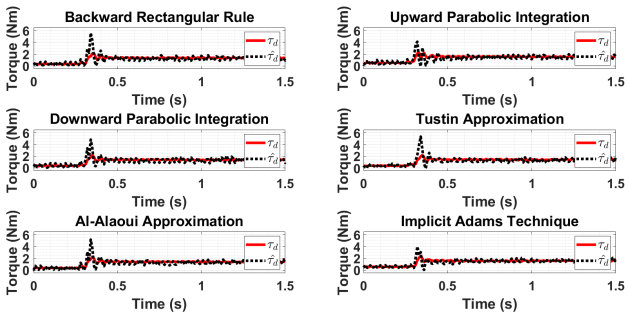

FIGURE 15. Scenario 2: Total disturbance estimation using six discrete-time approximations with $g_B = 20$ and $\alpha = 1$.

consistently demonstrates the most significant undershoot in speed response. Upon reviewing Figs. 14 and 15 collectively, it becomes evident that among the six techniques, two exhibit superior performance in reference speed tracking, while the

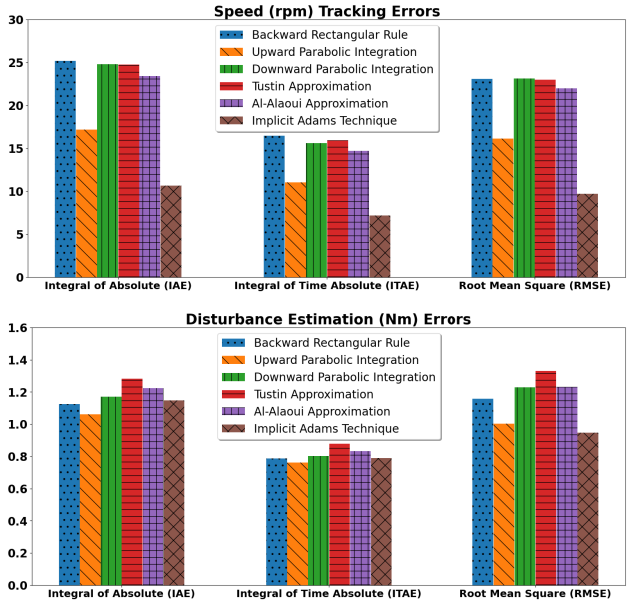

FIGURE 16. Scenario 3: Speed tracking findings using six discrete-time approximations with $g_B = 20$ and $\alpha = 2$.

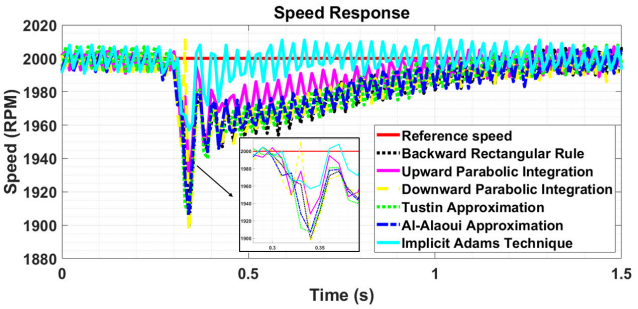

FIGURE 17. Scenario 3: Speed tracking findings using six discrete-time approximations with $g_B = 20$ and $\alpha = 2$.

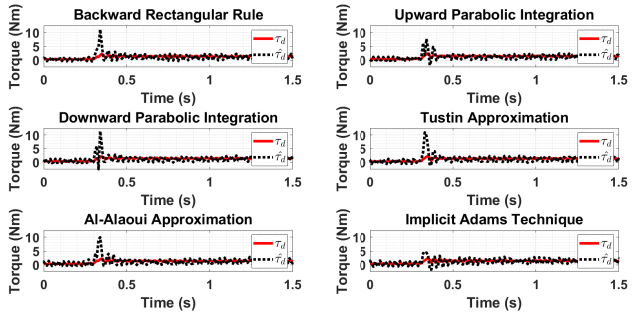

FIGURE 18. Scenario 3: Total disturbance estimation using six discrete-time approximations with $g_B = 20$ and $\alpha = 2$.

remaining four demonstrate slightly inferior and comparable performance in the presence of disturbances.

In Scenario 3, the system bandwidth remains consistent with Scenario 2 ($g_B = 20$), and parameter uncertainty increases ($\alpha = 2$). Examining the Speed Tracking (Fig. 17) after introducing a load at 0.3 seconds, implicit Adams stands out with the least undershoot (1957 rpm) and precise control system implementation. Another method with better performance is upward parabolic integration, albeit with a slightly higher undershoot (1928 rpm). On the contrary, downward parabolic integration displays the least favorable performance in terms of speed track, marked by a higher undershoot (1896 rpm). The results from Fig. 16 reveal the implicit Adams method's superior performance among the five disturbance estimation approximations, exhibiting the lowest value (4.2 Nm). The upward parabolic integration demonstrates commendable performance (7.7 Nm), while the least favorable outcome is observed with downward parabolic integration (11.39 Nm). In summary, the implicit Adams method emerges as the optimal choice, showcasing superior performance, accuracy, and speed for both disturbance estimation and speed tracking response, outperforming the other five techniques. Conversely, downward parabolic integration is discouraged due to its significantly inferior performance, nearly three times worse than the Adams method.

The findings in Table 7 offer a comprehensive comparison of error performances across three case experiments, examining the effectiveness of various discrete-time methods using three key evaluation criteria: Integral Absolute Error (IAE), Integral Time-weighted Absolute Error (ITAE), and Root Mean Square Error (RMSE). The assessment focuses on two critical categories: speed-tracking errors and disturbance estimation errors.

The table comprehensively assesses discrete-time methods across diverse conditions, meticulously scrutinizing their effectiveness in speed tracking and disturbance estimation across a spectrum of bandwidths (g_B) and parameter uncertainties (α). This thorough evaluation aims to offer insights into the methods' adaptability and robustness under varying scenarios, providing a nuanced understanding of their performance characteristics.

In the scenario with low bandwidth ($g_B = 10$, $\alpha = 1$), Downward Parabolic Integration demonstrated superior speed tracking, closely followed by Upward Parabolic Integration. Disturbance estimation indicated similar performance among most methods, with Implicit Adams slightly outperforming in ITAE while exhibiting comparable IAE values, except for Upward Parabolic Integration.

Under higher bandwidth ($g_B = 20$, $\alpha = 1$), Upward Parabolic Integration notably outperformed other methods in speed tracking, registering significantly lower errors. Implicit Adams followed as the second-best method, excelling across IAE, ITAE, and RMSE. In contrast, the Backward Rectangular Rule and Downward Parabolic Integration exhibited sub-optimal performance in speed tracking, while the Bilinear method showed promise in disturbance estimation.

However, when faced with scenarios marked by increased uncertainty, such as those defined by $g_B = 20$ and $\alpha = 2$, Implicit Adams emerges as a leading method in speed tracking, closely followed by Upward Parabolic Integration. Notably, Implicit Adams excels in providing superior Root Mean Square Error (RMSE) in disturbance estimation, showcasing its proficiency in handling uncertainties. Concurrently, Al-Alaoui exhibits commendable performance in terms of both Integral of Absolute Error (IAE) and Integral

TABLE 7. Error analysis of discrete-time methods in numerical approximations.

Discrete-Time-Method	Error	$g_B = 10, \alpha = 1$		$g_B = 20, \alpha = 1$		$g_B = 20, \alpha = 2$	
		Speed	Disturbance	Speed	Disturbance	Speed	Disturbance
Backward Rectangular Rule	IAE	24.18	0.23	17.65	0.42	25.67	1.13
	ITAE	15.41	0.16	10.8	0.27	16.48	0.79
	RMSE	23.01	0.22	17.63	0.49	23.09	1.28
Bilinear (Tustin) Approximation	IAE	19.1	0.23	15.82	0.31	24.76	1.28
	ITAE	12.07	0.16	9.95	0.21	15.95	0.88
	RMSE	18.155	0.22	15.62	0.38	22.98	1.33
Implicit Adams Second Order Hold	IAE	19.285	0.23	10.9	0.54	10.65	1.15
	ITAE	12.26	0.15	7.22	0.38	7.20	0.789
	RMSE	18.32	0.22	10.76	0.48	9.69	0.95
Al-Alaoui Method	IAE	18.21	0.23	15.99	0.42	23.42	1.22
	ITAE	11.41	0.16	9.67	0.28	14.72	0.83
	RMSE	17.75	0.22	15.98	0.45	21.98	1.23
Upward Parabolic Integration	IAE	17.94	0.25	9.53	0.43	17.19	1.06
	ITAE	10.54	0.16	5.78	0.28	11.04	0.76
	RMSE	17.99	0.24	10.82	0.42	16.15	1.00
Downward Parabolic Integration	IAE	16.2	0.23	17.41	0.45	24.80	1.17
	ITAE	9.95	0.16	11.21	0.32	15.63	0.80
	RMSE	16.28	0.23	16.53	0.46	23.14	1.23

of Time-weighted Absolute Error (ITAE), adding to the robustness of the overall approach in uncertain conditions.

This comparative analysis underscores the importance of method selection based on the nuances of application contexts. Specifically, downward parabolic integration exhibits favorable attributes for scenarios characterized by low bandwidth ratios. However, when dealing with situations resembling the given parameters of $g_B = 20$ and $\alpha = 1$, the use of upward parabolic integration consistently outperforms other methods in terms of speed tracking performance. Moreover, the distinct advantages observed in disturbance estimation through methods like implicit Adams approximation and bilinear approximation highlight their relevance in accurately estimating disturbances within the system. Overall, Implicit Adams consistently showcased robust performance across various bandwidth and uncertainty scenarios, excelling in speed and disturbance error evaluation. Upward Parabolic Integration displayed notable proficiency in speed tracking, whereas the Bilinear method exhibited competence in specific disturbance estimation contexts. These findings advocate for the practical application of Implicit Adams, particularly in digital DOB-based control, especially in contexts involving PMSMs.

V. DISCUSSION

This study delved into evaluating the effectiveness of different discrete-time methods for controlling PMSM across varying bandwidth ranges and parameter uncertainties. These factors were pivotal in distinguishing between the various approximation techniques utilized. The comprehensive assessment in Table 8 delves into the efficacy of various discrete-time methods within motion control systems.

Theoretical assessments involved stability analysis, employing open-loop transfer function calculations and the Bode integral theorem. Four methods were deemed unsuitable for PMSM motion control due to the identified waterbed effect and instability within the DOB. While methods like Al-Alaoui exhibit computational prowess, their applicability to highly intricate systems might be limited due to computational burdens.

Figure 19 represents the computational requirement for the discrete-time methods, which is found using the simulation of MATLAB/Simulink. Simulations are conducted using the computer with Intel Core i9- 7Gen processor and 32 GB RAM specifications. The computation time is indicated in microseconds (μs). The examination demonstrates that the Al-Alaoui technique displays the most lengthy processing time, with an amount of 5.625 μs. The backward rectangular rule is the quickest technique, which requires 1.758 μs. The Tustin approximation and upward parabolic integration approaches have similar execution times, around 2.7 μs each. The indicated computing time does not effect real-world implementation since the most effective methods do not have big differences in processing time. Furthermore, these findings can help selecting a suitable discretization approach based on specific application's requirements.

Despite the prevalent use of the Tustin approximation, its efficacy within the inner loop control of PMSMs showed

TABLE 8. Discrete-time-methods comparison.

Discrete-Time-Method	Stability	Waterbed Effect	Computational Complexity	Response Time	Robustness	Error Estimation
Forward Rectangular Rule	✓	✓	↓	×	×	×
Backward Rectangular Rule	✓	×	↓	○	↓	↓
Bilinear (Tustin) Approximation	✓	×	↓	↓	↑	↑
Implicit Adams Second Order Hold	✓	×	○	○	↑	↑
Simpson's Numerical Integration	×	×	↑	×	×	×
Al-Alaoui Method	✓	×	↑	○	○	○
Upward Parabolic Integration	✓	×	○	↑	○	↑
Downward Parabolic Integration	✓	×	↑	↓	↑	↑
Halijak Second Order Method	✓	✓	○	×	×	×
Tick Integration Rule	×	×	↑	×	×	×

*In which following signs stand for Stability: ✓ - BIBO Stable, × - BIBO Unstable, Waterbed Effect: ✓ - exist × - absent; Computational Complexity: ↑ - high level of computation, ○ - moderate level of computation, ↓ - low level of computation; Robustness × - eliminated method, Response time: × - eliminated method, ↑ - fast response, ○ - moderate response, ↓ - slow response; Robustness × - eliminated method, ↑ - low $K_{critical}$ value, ○ - moderate response, ↓ - high $K_{critical}$ value; Error estimation: × - eliminated method, ↑ - low error value, ○ - middle error value, ↓ - high error value.

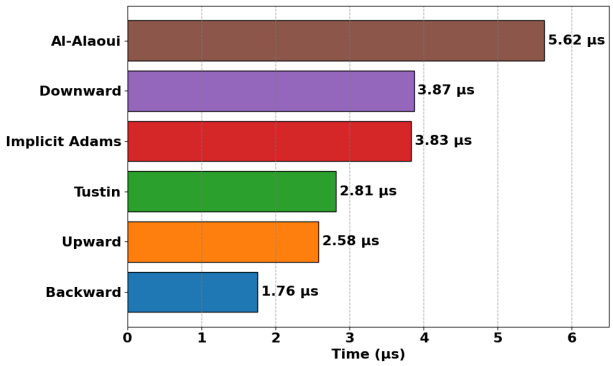

FIGURE 19. Processing time of various discretization methods.

suboptimal performance. Conversely, methods like upward parabolic integration and implicit Adams demonstrated promising post-response behaviors, indicating their potential suitability for applications requiring rapid response. Root locus analysis highlighted the robustness of implicit Adams, closely followed by the bilinear approach. In experimental observation, scenarios with low bandwidth ($g_B = 10$ and $\alpha = 1$) applications and six discrete time methods show successful performance in reference speed tracking with the maximum undershoot of 1895 rpm. In disturbance estimation error comparison, implicit Adams exhibited commendable performance across two parameters. At the same time, higher bandwidth scenarios ($g_B = 20$ and $\alpha = 2.5$) highlighted upward parabolic integration's prowess in speed error and the bilinear method's superior disturbance estimation are the next best methods after the implicit Adams second order hold technique.

Moreover, in speed response assessments, implicit Adams and upward parabolic integration demonstrated minimal undershoot, indicative of heightened stability—an advantageous trait for disturbance-sensitive high-performance digital control systems. These thorough theoretical and experimental studies shed light on the advantages and limits of discrete-time techniques in PMSM motion control applications. The results are relevant for technique selection, taking into account unique system difficulties, performance needs, and robustness considerations. Furthermore, the study's findings not only offer practical insights into control method selection, but they also serve as a springboard for future research. Incorporating DOBs into various motor system control strategies is an attractive subject for future research. The integration of more complex observer designs may pave the way for even greater levels of performance and control efficacy in motor control systems.

VI. CONCLUSION

This research examines the use of a digital DOB to improve the stability and performance of PMSM drive control systems. The theoretical assessments, together with practical data, highlight each method's nuanced strengths and limitations, underlining its suitability for complex systems. The highlighted limitations, such as the waterbed effect and instability within the DOB, highlight the importance of technique selection. While approaches such as Al-Alaoui are computationally powerful, they can also be used to construct reliable and robust control systems in digital platforms. Furthermore, the performance nuances shown by the Upward Parabolic Integration and Implicit Adams approaches indicate their potential appropriateness

for rapid-response applications, notwithstanding the limits discovered in specific situations.

Experimental results support theoretical conclusions, demonstrating that any of the six explored discrete-time approaches can be used to create control systems with a low bandwidth ratio. The robustness analyses show Implicit Adams as the clear winner in all frequency range situations, closely followed by upward parabolic integration in terms of stability and resilience to perturbations. This collective understanding emphasizes the importance of tailoring technique selection to account for system complexities, computational demands, and performance requirements. The findings serve as a compass for practitioners looking for optimal discrete-time approaches in PMSM motion control systems, allowing them to make more informed decisions that improve system efficiency, stability, and performance.

The study's conclusion highlights that the application of various discrete-time methods can enhance the robustness and accuracy of PMSM motion control systems. It also proposes the possibility of further research to investigate the utilization of DOBs in other types of motor control systems in future work, potentially incorporating more advanced observer designs to achieve even superior performance.

REFERENCES

[1] M. H. Vafaie, B. M. Dehkordi, P. Moallem, and A. Kiyoumarsi, "Improving the steady-state and transient-state performances of PMSM through an advanced deadbeat direct torque and flux control system," *IEEE Trans. Power Electron.*, vol. 32, no. 4, pp. 2964–2975, Apr. 2017.

[2] Y. Zuo, J. Mei, C. Jiang, X. Yuan, S. Xie, and C. H. T. Lee, "Linear active disturbance rejection controllers for PMSM speed regulation system considering the speed filter," *IEEE Trans. Power Electron.*, vol. 36, no. 12, pp. 14579–14592, Dec. 2021.

[3] E. Sariyildiz, R. Oboe, and K. Ohnishi, "Disturbance observer-based robust control and its applications: 35th anniversary overview," *IEEE Trans. Ind. Electron.*, vol. 67, no. 3, pp. 2042–2053, Mar. 2020.

[4] F. Chen, F. Lu, B. Jiang, and G. Tao, "Adaptive compensation control of the quadrotor helicopter using quantum information technology and disturbance observer," *J. Franklin Inst.*, vol. 351, no. 1, pp. 442–455, Jan. 2014.

[5] S. Yu, J. Wang, Y. Wang, and H. Chen, "Disturbance observer based control for four wheel steering vehicles with model reference," *IEEE/CAA J. Autom. Sinica*, vol. 5, no. 6, pp. 1121–1127, Nov. 2018.

[6] B. Sarsembayev, K. Suleimenov, and T. D. Do, "High order disturbance observer based PI-PI control system with tracking anti-windup technique for improvement of transient performance of PMSM," *IEEE Access*, vol. 9, pp. 66323–66334, 2021.

[7] C.-E. Ren, T. Du, G. Li, and Z. Shi, "Disturbance observer-based consensus control for multiple robotic manipulators," *IEEE Access*, vol. 6, pp. 51348–51354, 2018.

[8] M. Zheng, X. Lyu, X. Liang, and F. Zhang, "A generalized design method for learning-based disturbance observer," *IEEE/ASME Trans. Mechatronics*, vol. 26, no. 1, pp. 45–54, Feb. 2021.

[9] J. Ma, S.-L. Chen, C. S. Teo, A. Tay, A. Al Mamun, and K. K. Tan, "Parameter space optimization towards integrated mechatronic design for uncertain systems with generalized feedback constraints," *Automatica*, vol. 105, pp. 149–158, Jul. 2019.

[10] C. Dai, T. Guo, J. Yang, and S. Li, "A disturbance observer-based current-constrained controller for speed regulation of PMSM systems subject to unmatched disturbances," *IEEE Trans. Ind. Electron.*, vol. 68, no. 1, pp. 767–775, Jan. 2021.

[11] S. Singh and A. N. Tiwari, "Various techniques of sensorless speed control of PMSM: A review," in *Proc. 2nd Int. Conf. Electr., Comput. Commun. Technol. (ICECCT)*, Feb. 2017, pp. 1–6.

[12] E. Sariyildiz, S. Hangai, T. Uzunovic, T. Nozaki, and K. Ohnishi, "Stability and robustness of the disturbance observer-based motion control systems in discrete-time domain," *IEEE/ASME Trans. Mechatronics*, vol. 26, no. 4, pp. 2139–2150, Aug. 2021.

[13] N. Wan, D. Li, and N. Hovakimyan, "A simplified approach to analyze complementary sensitivity tradeoffs in continuous-time and discrete-time systems," *IEEE Trans. Autom. Control*, vol. 65, no. 4, pp. 1697–1703, Apr. 2020.

[14] K. Kong and M. Tomizuka, "Nominal model manipulation for enhancement of stability robustness for disturbance observer-based control systems," *Int. J. Control, Autom. Syst.*, vol. 11, no. 1, pp. 12–20, Feb. 2013.

[15] B. Wang, Z. Huo, Y. Yu, C. Luo, W. Sun, and D. Xu, "Stability and dynamic performance improvement of speed adaptive full-order observer for sensorless induction motor ultralow speed operation," *IEEE Trans. Power Electron.*, vol. 35, no. 11, pp. 12522–12532, Nov. 2020.

[16] N. F. O. Serteller, "Study the control analysis methods on a direct current motor," in *Proc. IEEE 29th Int. Symp. Ind. Electron. (ISIE)*, Jun. 2020, pp. 436–439.

[17] B. Spichartz and C. Sourkounis, "Design of a gain scheduling pitch controller for wind turbines by using the Bode diagram," in *Proc. 22nd IEEE Int. Conf. Ind. Technol. (ICIT)*, vol. 1, Mar. 2021, pp. 351–357.

[18] X. Yuan, J. Chen, C. Jiang, and C. H. T. Lee, "Discrete-time current regulator for AC machine drives," *IEEE Trans. Power Electron.*, vol. 37, no. 5, pp. 5847–5858, May 2022.

[19] W. Zhang, Z. Zhang, J. Lu, T. Chen, and Y. Li, "Back electromotive force-based discrete-time rotor position bias compensation method for permanent magnet synchronous motors," *IEEE Trans. Power Electron.*, vol. 38, no. 10, pp. 13030–13041, Oct. 2023.

[20] A. Urtasun, J. Samanes, E. L. Barrios, and P. Sanchis, "Control design and stability analysis of power converters: The discrete generalized Bode criterion," *IEEE Access*, vol. 9, pp. 37840–37854, 2021.

[21] Y. Zhang, Z. Yin, X. Cao, Y. Zhang, and J. Liu, "A novel SPMSM sensorless drive using discrete-time synchronous-frequency adaptive observer under low frequency ratio," *IEEE Trans. Power Electron.*, vol. 37, no. 9, pp. 11045–11057, Sep. 2022.

[22] F. Wang, K. Zuo, P. Tao, and J. Rodríguez, "High performance model predictive control for PMSM by using stator current mathematical model self-regulation technique," *IEEE Trans. Power Electron.*, vol. 35, no. 12, pp. 13652–13662, Dec. 2020.

[23] K. Yang, Y. Choi, and W. Kyun Chung, "Performance analysis of discrete-time disturbance observer for second-order systems," in *Proc. 42nd IEEE Int. Conf. Decis. Control*, Sep. 2003, pp. 4877–4882.

[24] A. Bernardini, P. Maffezzoni, and A. Sarti, "Linear multistep discretization methods with variable step-size in nonlinear wave digital structures for virtual analog modeling," *IEEE/ACM Trans. Audio, Speech, Language Process.*, vol. 27, no. 11, pp. 1763–1776, Nov. 2019.

[25] T. Ádám, S. Dadvandipour, and J. Futás, "Influence of discretization method on the digital control system performance," *Acta Montanistica Slovaca*, vol. 8, no. 4, pp. 197–200, 2003.

[26] K. Tschöke and H. Gravenkamp, "On the numerical convergence and performance of different spatial discretization techniques for transient elastodynamic wave propagation problems," *Wave Motion*, vol. 82, pp. 62–85, Nov. 2018.

[27] J. Menezes and T. Sands, "Discerning discretization for unmanned underwater vehicles DC motor control," *J. Mar. Sci. Eng.*, vol. 11, no. 2, p. 436, Feb. 2023.

[28] R. L. Burden, J. D. Faires, and M. Annette, *Burden. Numerical Analysis*, vol. 10. Boston, MA, USA: Cengage Learning Inc, 2016.

[29] J. T. Machado, "Analysis and design of fractional-order digital control systems," *Syst. Anal. Model. Simul.*, vol. 27, nos. 2–3, pp. 107–122, 1997.

[30] M. A. Al-Alaoui, "Novel digital integrator and differentiator," *Electron. Lett.*, vol. 29, no. 4, p. 376, 1993.

[31] F. Vatansever and M. Hatun, "S-to-Z transformation tool for discretization," *Gazi Univ. J. Sci. C, Design Technol.*, vol. 9, no. 4, pp. 773–783, 2021.

[32] C. A. Halijak, "Digital simulation of continuous feedback systems," *Comput. Electr. Eng.*, vol. 1, no. 3, pp. 453–457, Dec. 1973.

[33] D. V. Griffiths and I. M. Smith, *Numerical Methods for Engineers*. Boca Raton, FL, USA: CRC Press, 2006.

[34] W. Richard, "Hamming. digital filters," in *Signal Processing Series*. Upper Saddle River, NJ, USA: Prentice-Hall, 1989.

[35] Y. Han, H. Sun, B. Huang, and S. Qin, "Discrete-time domain modal analysis of oscillatory stability of renewables integrated power systems," *IEEE Trans. Power Del.*, vol. 37, no. 5, pp. 4248–4260, Oct. 2022.
[36] M. Ruth, K. Lebsock, and C. Dennehy, "What's new is what's old: Use of Bode's integral theorem (circa 1945) to provide insight for 21st century spacecraft attitude control system design tuning," in *Proc. AIAA Guid., Navigat., Control Conf.*, Aug. 2010, p. 8428.
[37] A. Emami-Naeini and D. de Roover, "Bode's sensitivity integral constraints: The waterbed effect revisited," 2019, *arXiv:1902.11302*.
[38] S. Bittanti and P. Colaneri, *Periodic Systems: Filtering and Control*, vol. 5108985. Cham, Switzerland: Springer, 2009.

KULASH TALAPIDEN received the B.S. degree (Hons.) in technological machinery and equipment from Kazakh Agrotechnical University, in 2020, Astana, Kazakhstan, and the M.S. degree in robotics from the School of Engineering and Digital Sciences, Nazarbayev University, Astana. Since 2022, she has been a Research Assistant with the Power Conversion and Motion Control (PCMC) Laboratory for Motion Control Systems, School of Engineering and Digital Sciences, Nazarbayev University. Her research interests include control systems, feedback control in motor drives, and robotics applications.

YUSSUF SHAKHIN received the B.S. degree in electronics and nanoelectronics engineering from Ala-Too International University, Kyrgyzstan, in 2021, and the M.S. degree in robotics from Nazarbayev University, Kazakhstan, in 2023, where he is currently pursuing the Ph.D. degree with the Department of Robotics and Mechatronics. Since 2021, he has been with the Power Conversion and Motion Control (PCMC) Laboratory for Motion Control Systems. Additionally, from 2022 to 2023, he was a Research Assistant with the Smart Energy Laboratory for Wireless Power Transfer Systems, School of Engineering and Digital Sciences, Nazarbayev University. His current research interests include the control of electric machine drives employed in electric vehicles and mobile robots.

NGUYEN GIA MINH THAO (Senior Member, IEEE) received the B.Eng. degree (Hons.) in electrical and electronics engineering from Vietnam National University–Ho Chi Minh City University of Technology, Vietnam, in 2009, and the Dr.-Eng. degree in electrical engineering and intelligent control from Waseda University, Tokyo, Japan, in 2015. From 2015 to 2020, he was a Postdoctoral Researcher with Waseda University and Toyota Technological Institute, Japan. From 2020 to 2023, he was an Assistant Professor with Nagoya University and Toyota Technological Institute. Since 2023, he has been an Associate Professor with Shimane University, Japan, where he is currently the Head of the Electric Motors and Energy Systems Laboratory. His research interests include advanced control methods, electric motors and drives, power electronics, electromagnetic analysis and evaluation, renewable energy, optimization, and electric vehicles. He has been an Associate Editor of IEEE TRANSACTIONS ON INDUSTRY APPLICATIONS, since 2022. He has been the Guest Editor of Special Issues on refereed journals, such as *Electronics* and *The Journal of Engineering* (IET). Moreover, he has been an Editorial Member of the *Journal of Computer Science and Cybernetics*, since 2021.

TON DUC DO (Senior Member, IEEE) received the B.S. and M.S. degrees from Hanoi University of Science and Technology, Hanoi, Vietnam, in 2007 and 2009, respectively, and the Ph.D. degree from Dongguk University, Seoul, South Korea, in 2014, all in electrical engineering.

From 2008 to 2009, he was with the Division of Electrical Engineering, Thuy Loi University, Vietnam, as a Lecturer. He was with the Division of Electronics and Electrical Engineering, Dongguk University, as a Postdoctoral Researcher, in 2014. He was also a Senior Researcher with the Pioneer Research Center for Controlling Dementia by Converging Technology, Gyeongsang National University, South Korea, from May 2014 to August 2015. Since September 2015, he has been an Assistant Professor and then an Associate Professor with the Department of Robotics and Mechatronics, Nazarbayev University, Kazakhstan. His research interests include the field of control engineering, electric drives, renewable energy conversion systems, and nanorobots. He received the Best Research Award from Dongguk University in 2014, the Most Cited Paper Award from Wind Energy in 2020-2021, and the Outstanding Associate Editor Award of IEEE ACCESS in 2021 and 2022. He has been listed in the top 2% of scientists based on the citation on the single-year table in 2020 and 2021, and both single-year and career-wide tables in 2021, 2022, and 2023. He has been an Associate Editor of IEEE ACCESS, since April 2017, and IEEE ROBOTICS AND AUTOMATION LETTERS, since August 2023. He has been recently promoted to a Senior Editor of IEEE ACCESS. He has been the Guest Editor of Special Issues on several journals, such as *Mathematical Problems in Engineering*, *Electronics*, *Energies*, *Sensors*, and *Fractal and Fractional*.